**Supplementary Information**

# Bidirectional Crosstalk between MAOA and AR Promotes Hormone-Dependent and Castration-Resistant Prostate Cancer

**Jing Wei, Lijuan Yin, Jingjing Li, Jing Wang, Tianjie Pu, Peng Duan, Tzu-Ping Lin, Allen C. Gao, and Boyang Jason Wu**

| Dataset | *PSA* | *TMPRSS2* | *FKBP5* | Reference |
|---|---|---|---|---|
| Grasso (n=94) | 0.65 ** | 0.49 ** | 0.03 | (1) |
| Bittner (n=60) | 0.66 ** | 0.36 ** | 0.10 | NA |
| Holzbeierlein (n=50) | 0.35 * | 0.23 | 0.37 * | (2) |
| Wallace (n=69) | 0.38 ** | 0.49 ** | 0.33 ** | (3) |
| Luo 2 (n=15) | 0.08 | 0.78 ** | 0.69 ** | (4) |
| Vanaja (n=32) | 0.56 ** | 0.63 ** | 0.65 ** | (5) |
| Welsh (n=25) | -0.28 | 0.23 | 0.18 | (6) |
| Taylor 3 (n=155) | 0.34** | 0.45 ** | 0.38 ** | (7) |
| Yu (n=88) | 0.49 ** | 0.56 ** | 0.53 ** | (8) |
| True (n=31) | -0.20 | 0.12 | 0.03 | (9) |
| Arredouani (n=13) | -0.01 | 0.00 | -0.41 | (10) |
| LaTulippe (n=32) | 0.36 * | 0.58 ** | 0.21 | (11) |
| Lapointe (n=71) | 0.10 | 0.19 | 0.40 ** | (12) |
| Nanni (n=22) | -0.51 * | 0.19 | 0.15 | (13) |
| Setlur (n=363) | 0.07 | NA | 0.02 | (14) |
| Singh (n=52) | -0.13 | 0.40 ** | 0.21 | (15) |
| Glinsky (n=79) | 0.12 | 0.27 * | 0.20 | (16) |
| Setlur 2 (n=109) | 0.39 ** | NA | 0.15 | (14) |
| Liu (n=44) | 0.06 | 0.32 * | 0.31 * | (17) |
| Tamura (n=35) | 0.01 | -0.21 | 0.39 * | (18) |
| Best 2 (n=20) | 0.05 | 0.25 | -0.27 | (19) |
| Chandran (n=31) | -0.04 | -0.05 | NA | (20) |
| Varambally (n=13) | 0.68 * | 0.78 ** | 0.71 ** | (21) |
| Robinson (n=118) | 0.32 ** | 0.38 ** | 0.34 ** | (22) |
| Kumar (n=176) | 0.57 ** | 0.32 ** | 0.30 * | (23) |
| TCGA (n=498) | 0.12 ** | 0.28 ** | 0.13 ** | (24) |
| Beltran (n=114) | 0.35 * | 0.47 ** | 0.17 | (25) |
| Abida (n=444) | 0.25 ** | 0.38 ** | 0.22 ** | (26) |
| Ren (n=65) | 0.47 ** | 0.59 ** | 0.17 | (27) |
| Barbieri (n=31) | 0.05 | -0.09 | 0.09 | (28) |
| Gerhauser (n=324) | 0.28 ** | 0.19 * | -0.02 | (29) |

**Supplementary Table S1. Co-expression correlation analysis of *MAOA* with *PSA*, *TMPRSS2* and *FKBP5* mRNA in clinical PC datasets.** All datasets are available in the Oncomine or cBioPortal databases and were analyzed by Pearson correlation with Pearson's *r* indicated. **p*<0.05, ***p*<0.01.

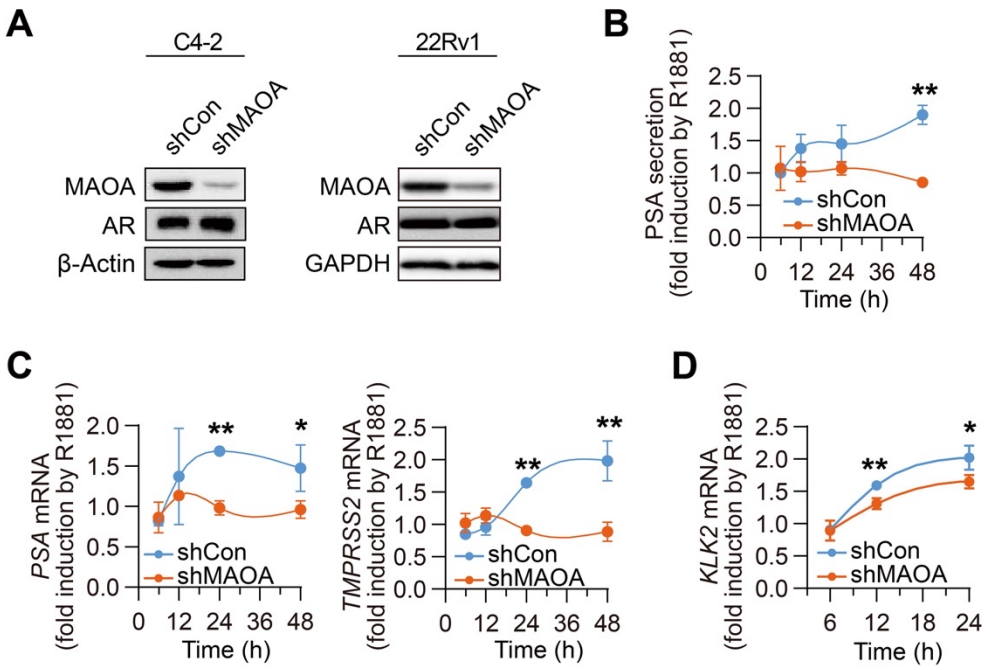


**Supplementary Figure S1. MAOA silencing reduced AR transcriptional activity in CRPC cells. (A)** Western blot of MAOA and AR in control (shCon) and MAOA-KD (shMAOA) C4-2 and 22Rv1 cells. **(B)** ELISA of time-dependent fold induction of PSA secretion by R1881 (10 nM) in control and MAOA-KD C4-2 cells (*n*=3). **(C)** qPCR of time-dependent fold induction of *PSA* and *TMPRSS2* by R1881 (10 nM) in control and MAOA-KD C4-2 cells (*n*=3). **(D)** qPCR of time-dependent fold induction of *KLK2* by R1881 (10 nM) in control and MAOA-KD 22Rv1 cells (*n*=3). Data represent the mean ± SEM. **p*<0.05, ***p*<0.01.

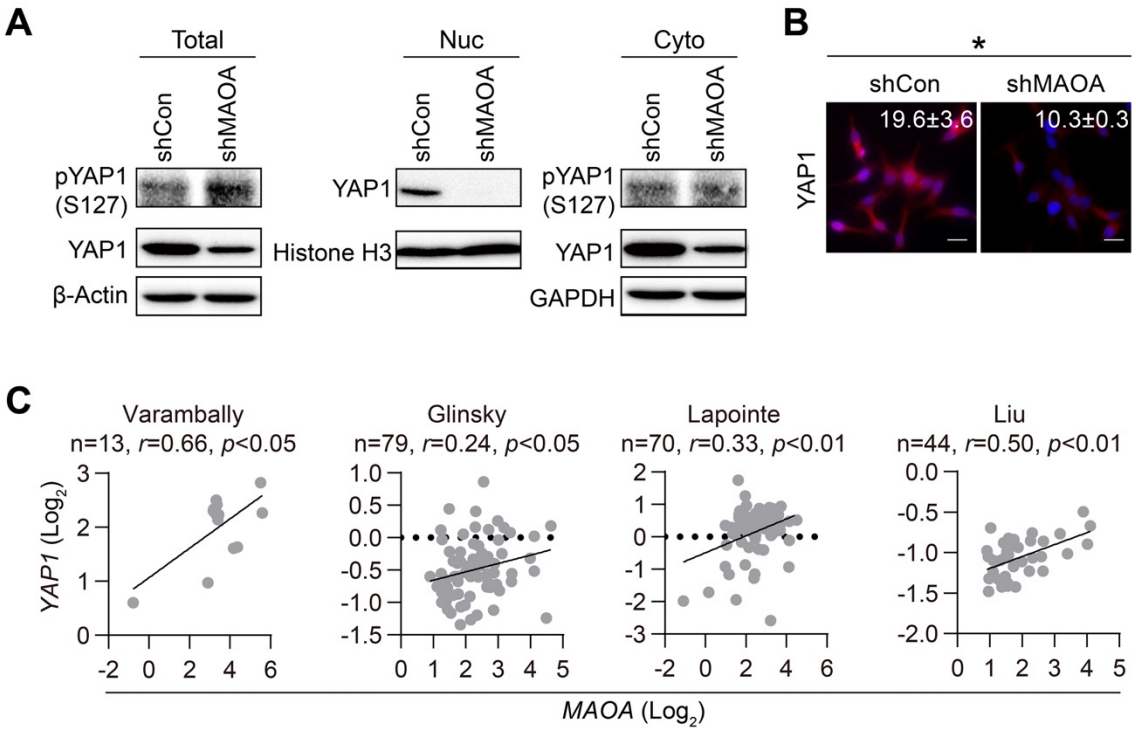


**Supplementary Figure S2. MAOA upregulates YAP1 in PC cells. (A)** Western blot of YAP1 and phospho-YAP1 (S127) in total cell lysates along with nuclear and cytoplasmic fractions of control and MAOA-KD 22Rv1 cells. **(B)** Representative YAP1 staining and quantification of per-nucleus intensity in control (*n*=170) and MAOA-KD (*n*=115) C4-2B$^{ENZR}$ cells. Scale bars: 20 μm. **(C)** Pearson correlation analysis of *MAOA* and *YAP1* in 4 PC clinical datasets. Data represent the mean ± SEM. **p*<0.05.

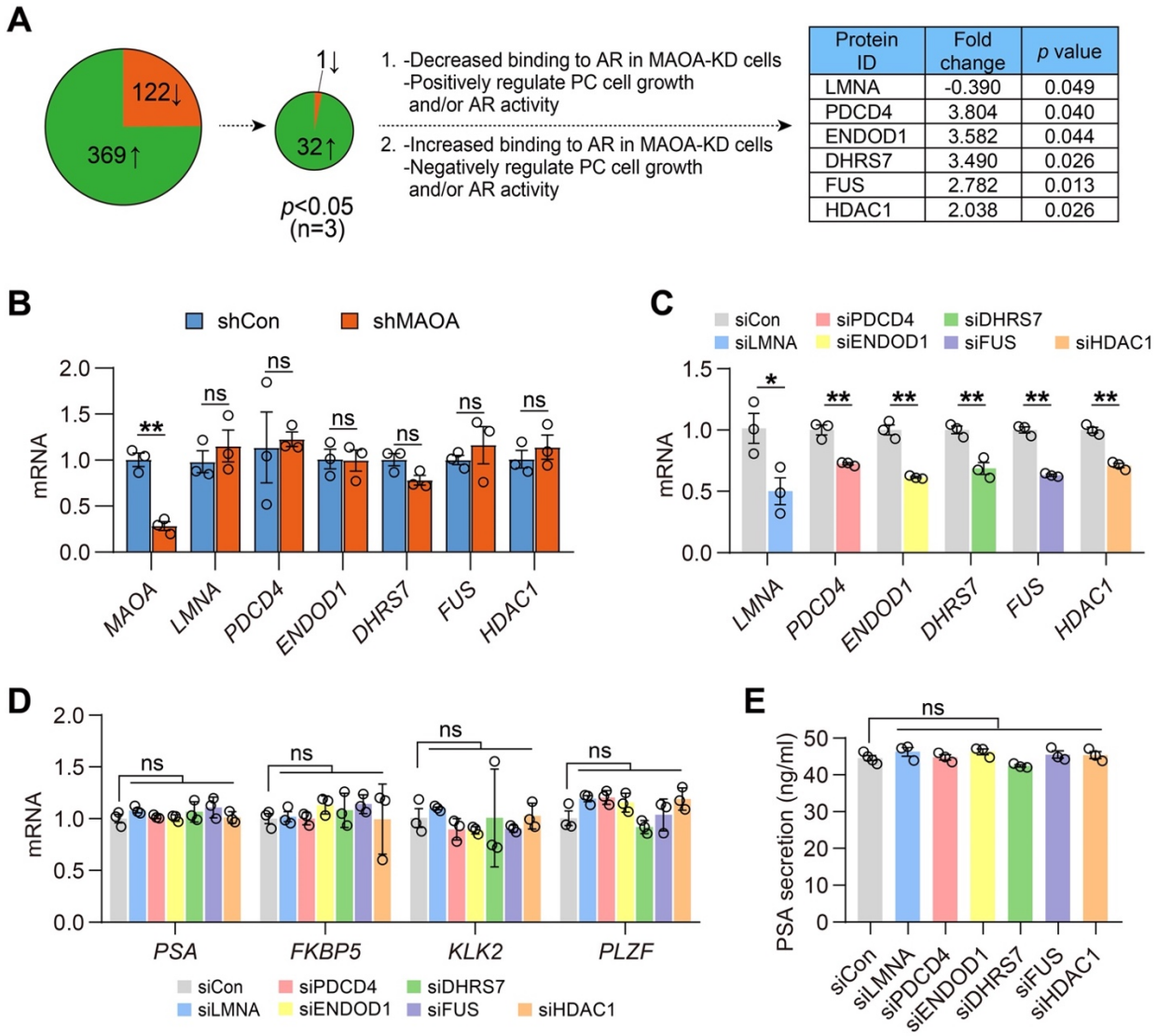


| Protein ID | Fold change | *p* value |
|---|---|---|
| LMNA | -0.390 | 0.049 |
| PDCD4 | 3.804 | 0.040 |
| ENDOD1 | 3.582 | 0.044 |
| DHRS7 | 3.490 | 0.026 |
| FUS | 2.782 | 0.013 |
| HDAC1 | 2.038 | 0.026 |

**Supplementary Figure S3. Mass spectrometry-based proteomic analysis of MAOA's effect on AR interaction with AR partner proteins in PC cells. (A)** Schematic summary of the mass spectrometric analysis for identification of AR nuclear interactors with differential AR-binding degrees in MAOA-KD LNCaP cells compared to controls. High-confidence candidate AR-interacting proteins expressed in the nucleus and reported to play a regulatory role in PC cell growth and/or AR activity, as listed in the table, were analyzed further. See also Supplementary Dataset S1. **(B)** qPCR of *MAOA* and candidate AR interactor genes in control and MAOA-KD LNCaP cells (*n*=3). **(C)** qPCR of candidate AR interactor genes in LNCaP cells treated with control siRNA (siCon) or siRNAs against individual genes as indicated (*n*=3). **(D, E)** Analysis of AR target genes by qPCR (D) and PSA secretion by ELISA (E) in LNCaP cells treated with control siRNA or siRNAs against individual candidate AR interactor genes as indicated (*n*=3). Data represent the mean ± SEM. **p*<0.05, ***p*<0.01; ns, not significant.

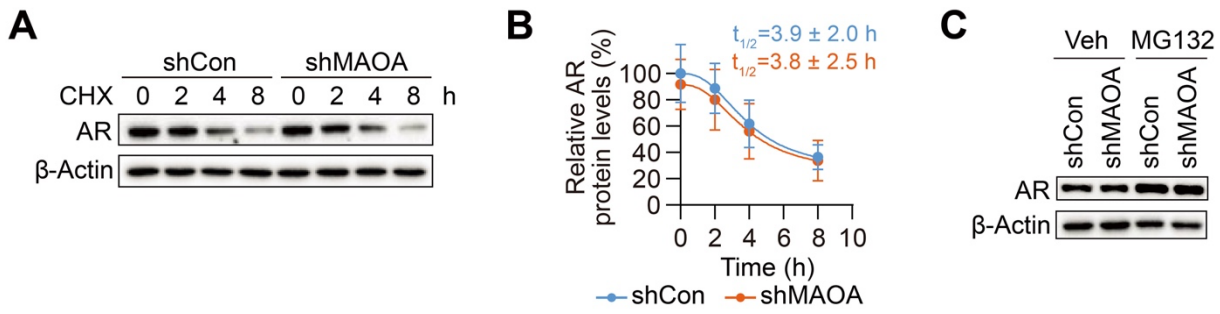


**Supplementary Figure S4. MAOA exerts no effect on AR protein stability in PC cells. (A)** Western blot of AR in control and MAOA-KD LNCaP cells under cycloheximide (CHX, 50 μg/ml) treatment for different times. **(B)** Quantitation of AR levels normalized to β-Actin in control and MAOA-KD LNCaP cells from 3 independent experiments described in (A), with the average AR half-life from each group shown on top. The AR/β-Actin ratio at 0 hr is set as 100% in each group. **(C)** Western blot of AR by MG132 (10 μM, 8 hrs) in control and MAOA-KD LNCaP cells. Data represent the mean ± SEM.

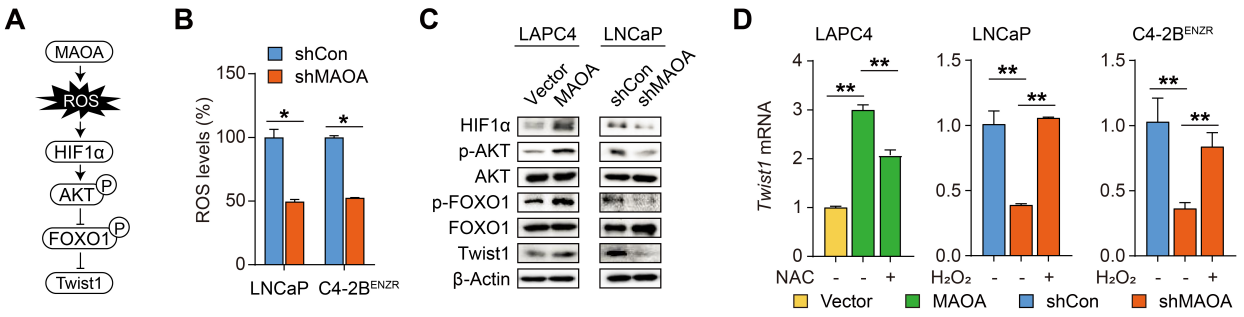


**Supplementary Figure S5. MAOA activates Twist1 through ROS in AR-positive PC cells.** **(A)** A model summarizing the reported MAOA-ROS-Twist1 axis in PC cells (30). **(B)** Flow cytometric analysis of intracellular ROS levels in control and MAOA-KD LNCaP and C4-2B$^{ENZR}$ cells ($n$=3). The ROS levels in control cells are set as 100%. **(C)** Western blot of HIF1α, p-AKT (Ser473), total AKT, p-FOXO1 (Ser256), total FOXO1 and Twist1 in the indicated control and MAOA-manipulated cells. **(D)** qPCR of *Twist1* in the indicated control and MAOA-manipulated cells under treatment of N-acetylcysteine (NAC, 10 mM, 24 hrs) or $H_2O_2$ (20 μM, 2 hrs) ($n$=3). Data represent the mean ± SEM. *$p$<0.05, **$p$<0.01.

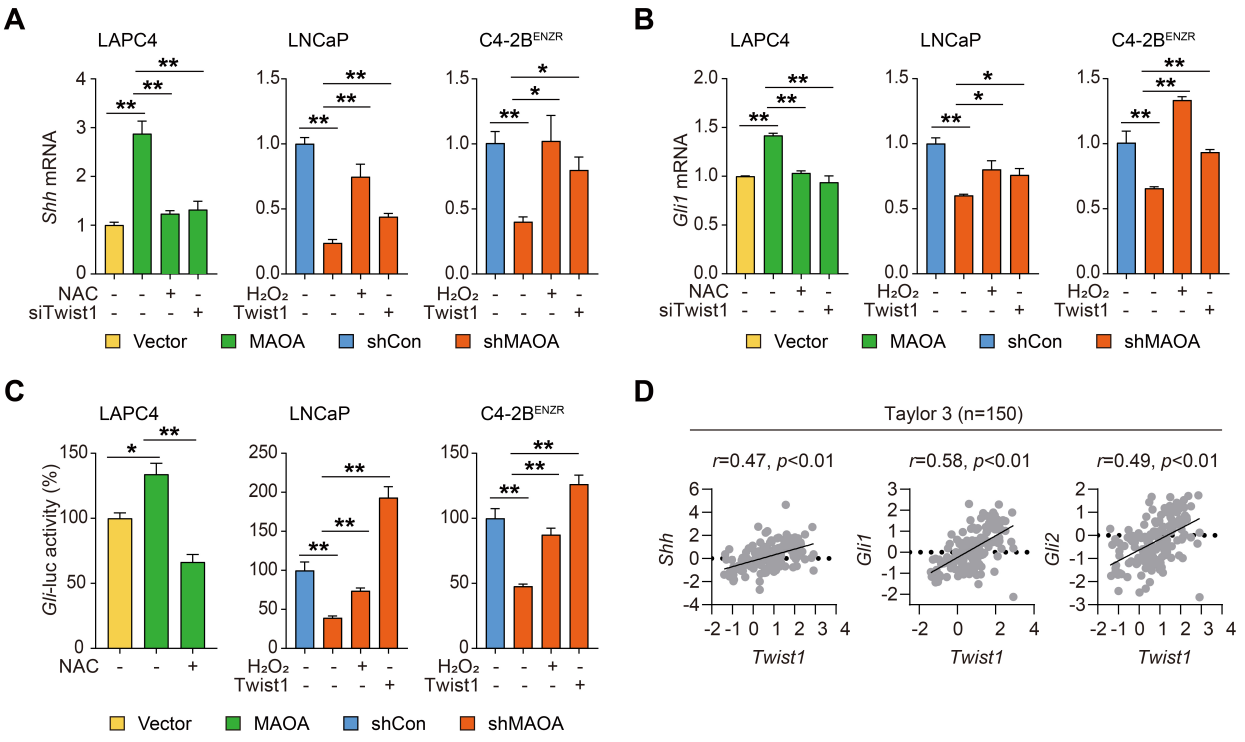


**Supplementary Figure S6. MAOA induces Shh/Gli signaling depending on ROS and Twist1 in AR-positive PC cells. (A, B)** qPCR of *Shh* (A) and *Gli1* (B) in the indicated control and MAOA-manipulated cells modified for intracellular ROS (NAC, 10 mM, 24 hrs; $H_2O_2$, 20 μM, 2 hrs) or Twist1 levels (*n*=3). **(C)** Determination of Gli-responsive luciferase reporter (Gli-luc) activity in the indicated control and MAOA-manipulated cells with modified levels of ROS or Twist1 as described in (A, B) (*n*=3). **(D)** Pearson correlation analysis of *Twist1* with *Shh, Gli1* and *Gli2* in the Taylor 3 dataset. Data represent the mean ± SEM. **p*<0.05, ***p*<0.01.

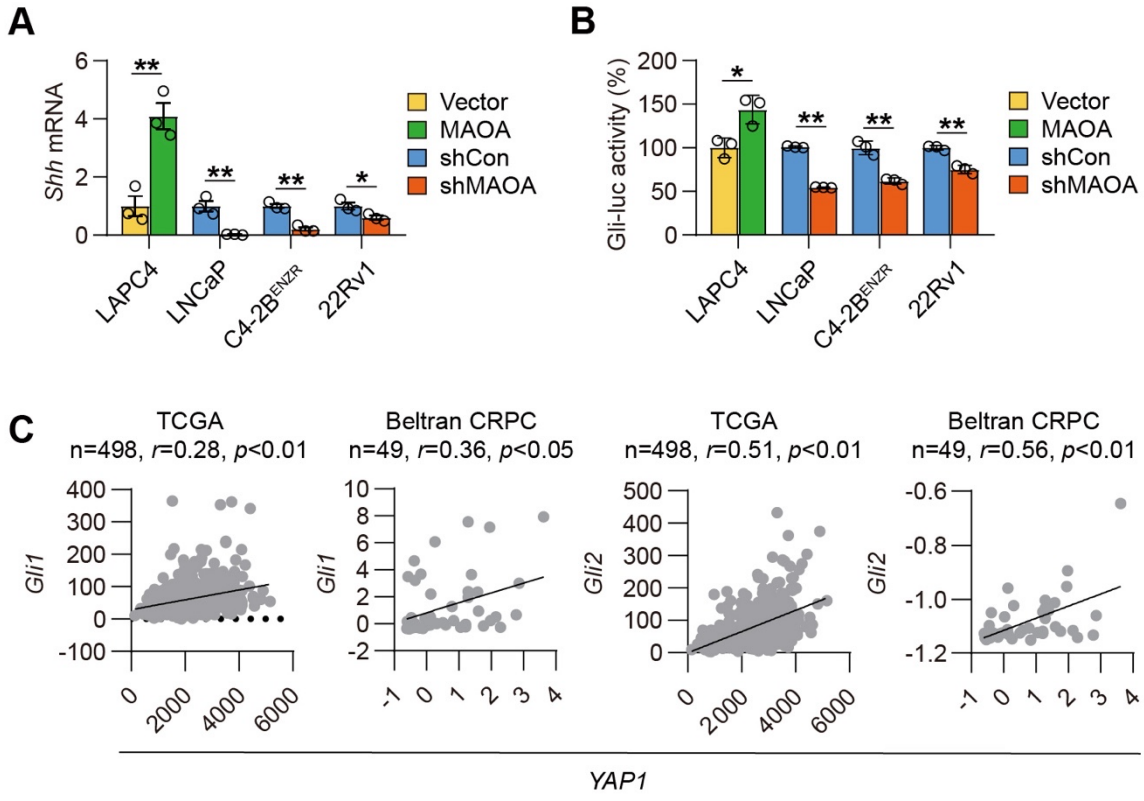


**Supplementary Figure S7. MAOA activates YAP1 through Shh/Gli signaling. (A, B)** Analysis of *Shh* by qPCR (A) and Gli-luc activity by dual-luciferase reporter assays (B) in the indicated control and MAOA-manipulated cells ($n$=3). **(C)** Pearson correlation analysis of *YAP1* with *Gli1* and *Gli2* in the TCGA and Beltran datasets. Data represent the mean ± SEM. *$p$<0.05, **$p$<0.01.

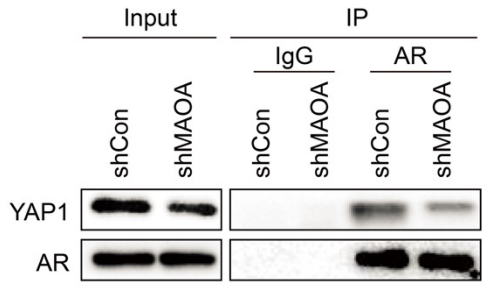


**Supplementary Figure S8. MAOA silencing reduced YAP1-AR interaction in PC cells.** Co-IP assays of YAP1-AR interaction in whole cell lysates of control and MAOA-KD LNCaP cells. IgG was used in the IP step as negative control. Five-percent input was blotted as positive control.

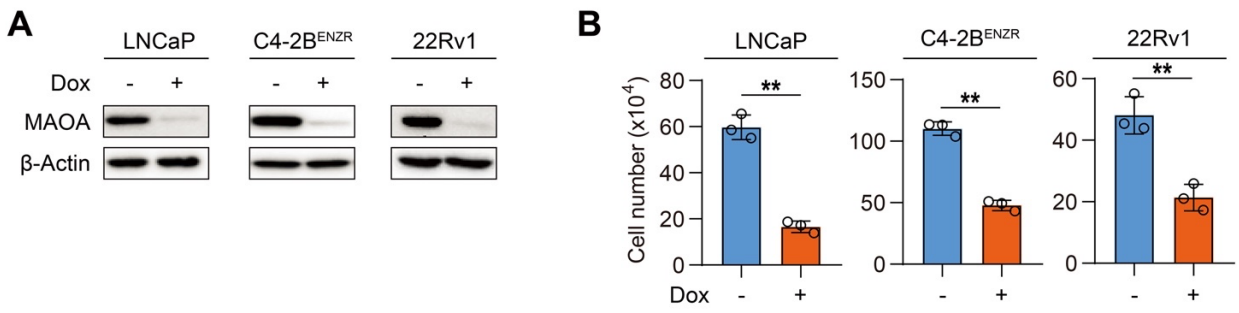


**Supplementary Figure S9. Validation of Dox-inducible *MAOA* shRNA in PC cells. (A)** Western blot of MAOA in LNCaP, C4-2B$^{ENZR}$ and 22Rv1 cells stably expressing Dox-inducible *MAOA* shRNA upon Dox stimulation (100 ng/ml, 72 hrs). **(B)** Cell counting assays in parallel with (A) (*n*=3). Data represent the mean ± SEM. ***p*<0.01.

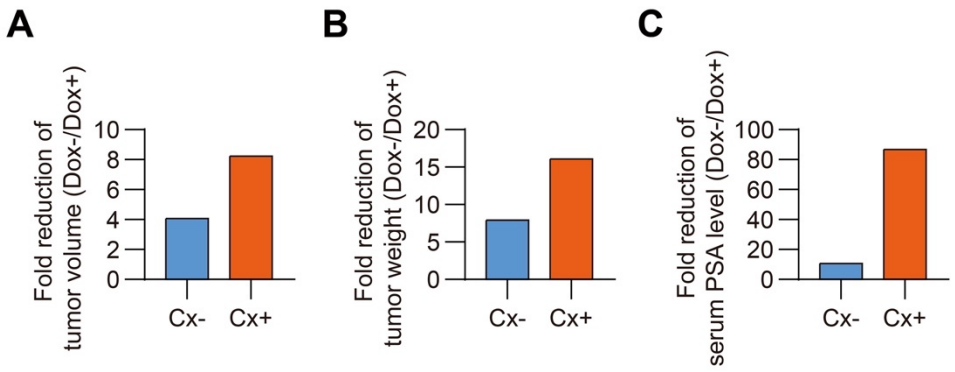


**Supplementary Figure S10. MAOA knockdown resulted in a greater fold reduction of tumor growth in castration-resistant tumors than hormone-naïve tumors in a LNCaP xenograft model. (A-C)** Comparisons of fold reductions (Dox-/Dox+) in average endpoint tumor volume (A), tumor weight (B), and serum PSA level (C) caused by Dox-induced tumor MAOA silencing in castrated (Cx+) and intact (Cx-) mice.

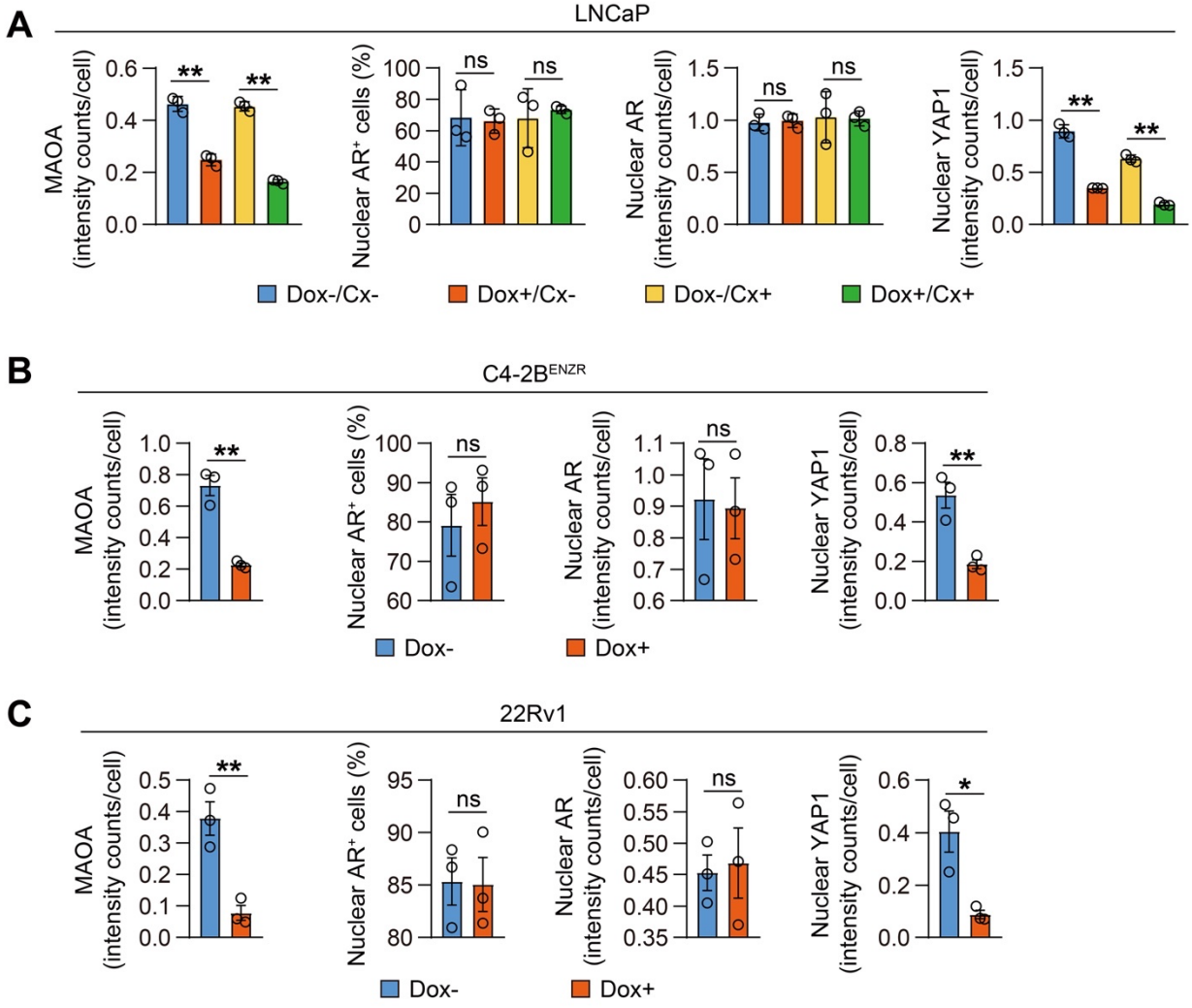


**Supplementary Figure S11. Quantitative IHC analysis of MAOA, AR and YAP1 protein expression in xenograft tumors. (A-C)** Quantitative analysis of per-cell IHC staining intensity of MAOA, nuclear AR and nuclear YAP1, and the percentage of nuclear AR$^+$ cells in LNCaP (A, *n*=3), C4-2B$^{ENZR}$ (B, *n*=3) and 22Rv1 (C, *n*=3) xenograft tumors.

## Supplementary Materials and Methods

### Cell culture

All PC cell lines were maintained in RPMI-1640 medium (Corning) supplemented with 10% FBS (Atlanta Biologicals) and 1% penicillin/streptomycin (Corning). The C4-2B$^{ENZR}$ cell line was cultured further in the continuous presence of 20 μM Enz to maintain Enz resistance. The 293T cell line was maintained in DMEM medium (Corning) supplemented with 10% FBS and 1% penicillin/streptomycin.

### Plasmids, antibodies and reagents

The human *PSA* enhancer-promoter fused *Firefly* luciferase reporter *PSA*-luc was provided by Gerhard Coetzee (Van Andel Research Institute) (31). A human 1.6-kb *YAP1* promoter *Gaussia* luciferase reporter that simultaneously expresses secreted alkaline phosphatase (SEAP) as internal control for normalization of transfection efficiency was purchased from GeneCopoeia. The YAP/TAZ-responsive *Firefly* luciferase reporter 8xGTIIC-luc was obtained from Addgene. The pRL-TK *Renilla* luciferase reporter was obtained from Promega. The Gli-responsive *Firefly* luciferase reporter Gli-luc was provided by Hiroshi Sasaki (RIKEN Center for Developmental Biology) (32) and obtained from the RIKEN Bioresource Center. Human pcDNA3.1-FLAG-Twist1 expression construct was provided by Anthony Firulli (Indiana University) (33). Human *LMNA*, *PDCD4*, *ENDOD1*, *DHRS7*, *FUS*, *HDAC1*, *Twist1* and non-target control siRNAs were purchased from Santa Cruz. Primary antibodies against MAOA (H-70, Santa Cruz, RRID: AB_2137260 or G-10, Santa Cruz, RRID: AB_10609510), PSA (C-19, Santa Cruz, RRID: AB_2134513), AR (N-20, Santa Cruz, RRID: AB_1563391 or 441, Santa Cruz, RRID: AB_626671), p-YAP1 (Ser127, D9W2I, Cell Signaling, RRID: AB_2650553), YAP1 (63.7, Santa Cruz, RRID: AB_1131430), Histone H3 (D1H2, Cell Signaling, RRID: AB_10544537), GAPDH (14C10, Cell Signaling, RRID: AB_10693448), β-Actin (AC-15, Santa Cruz, RRID: AB_1119529), HIF1α (clone 54, Biosciences, RRID: AB_398271), p-AKT (Ser473, D9E, Cell Signaling, RRID: AB_2315049), AKT (C67E7, Cell Signaling, RRID: AB_915783), p-FOXO1 (Ser256, Cell Signaling, RRID: AB_329831), FOXO1 (C29H4, Cell Signaling, RRID: AB_2106495), or Twist1 (Sigma-Aldrich, RRID: AB_609890) were purchased from different commercial vendors. Cycloheximide, MG132, N-acetylcysteine (NAC) and hydrogen peroxide ($H_2O_2$) were purchased from Sigma-Aldrich.

### Generation of stable knockdown and overexpression cells

Stable shRNA-mediated MAOA KD was achieved by infecting cells with lentiviral particles expressing *MAOA* shRNA TRCN0000046009 (shMAOA), followed by 2-week puromycin selection (2 μg/ml) to establish stable cell lines. A non-target control shRNA (shCon) was used as control for stable KD cells. Lentivirus production was performed to stably overexpress MAOA in LAPC4 cells and Dox-inducible *MAOA* shRNA in LNCaP, C4-2B$^{ENZR}$ and 22Rv1 cells. Briefly, 293T cells were co-transfected with a *MAOA*- or Dox-inducible *MAOA* shRNA-expressing lentiviral construct, pCMV delta R8.2 (Addgene) and pVSVG (Addgene) in a 4:2:1 ratio using Lipofectamine 2000 reagent (Thermo Fisher Scientific) following the manufacturer's instructions. The medium was changed 6 hours after transfection. The medium containing lentivirus was harvested 48 hours after transfection. Viral particles were concentrated and purified using a Lenti-X concentrator (Takara Bio). PC cells were infected with lentivirus in the presence of 8 μg/ml polybrene followed by 2-week puromycin selection (2 μg/ml). An empty lentiviral construct was used as control for stable OE of MAOA in LAPC4 cells.

### Quantitative real-time PCR

qPCR was conducted using SYBR Green PCR Master Mix and run with the Applied Biosystems QuantStudio 3 Real-Time PCR System (Thermo Fisher Scientific). PCR conditions

included an initial denaturation step of 10 min at 95°C, followed by 40 cycles of PCR consisting of 15 s at 95°C and 1 min at 60°C. The PCR data were analyzed by the $2^{-\Delta\Delta CT}$ method (34).

| Gene | Forward | Reverse |
|---|---|---|
| *MAOA* | CTGATCGACTTGCTAAGCTAC | ATGCACTGGATGTAAAGCTTC |
| *AR* | CTGATCGACTTGCTAAGCTAC | ATGCACTGGATGTAAAGCTTC |
| *PSA* | CCAGAGGAGTTCTTGACCCCAAA | CCCCAGAATCACCCGAGCAG |
| *FKBP5* | CGGAGAACCAAACGGAAAGG | CTTCGCCCACAGTGAATGC |
| *KLK2* | AGCCTGCCAAGATCACAGAT | GCAAGAACTCCTCTGGTTCG |
| *PLZF* | CTATGGGCGAGAGGAGAGTG | TCAATACAGCGTCAGCCTTG |
| *TMPRSS2* | TAGTGAAACCAGTGTGTCTGCCCA | AGCGTTCAGCACTTCTGAGGTCTT |
| *CTGF* | CCTGCAGGCTAGAGAAGCAG | TGGAGATTTTGGGAGTACGG |
| *IGFBP3* | GGGGTGTACACATTCCCAAC | AGGCTGCCCATACTTATCCA |
| *AMOTL2* | AGGAGGCTGCAAGACTTCAA | AGCTTCTCTTGCTCCTGCTG |
| *Cyr61* | GAGGGCAGACCCTGTGAATA | GTTCTTGGGGACACAGAGGA |
| *GATA3* | GTCCTGTGCGAACTGTCAGA | TTTCTGGTCTGGATGCCTTC |
| *YAP1* | TAGCCCTGCGTAGCCAGTTA | TCATGCTTAGTCCACTGTCTGT |
| *ETV1* | TACCCCATGGACCACAGATT | TAAAGCCTTGTGGTGGGAAG |
| *ETS1* | CCAATCCAGCTATGGCAGTT | TTCCTCTTTCCCCATCTCCT |
| *ARID5A* | GATGCCAGGAAAGACCAAAG | GCTTGTAGGCCTCAGGACAG |
| *PSMC3IP* | ACAGCTCCCAGGATGTGTTC | GGTCCTGATCCGCAAAATAG |
| *DCAF6* | GAAGCAAGTGAGGTTGCACA | GACTTGATGGGACCGTAGGA |
| *FOXA2* | GTATGCTGGGAGCCGTGAAG | AGCCTGCGCTCATGTTGC |
| *NR5A1* | GAGAGCCAGAGCTGCAAGAT | CTTGTACATCGGCCCAAACT |
| *TRIP4* | CCAGAAGCACAAGCTCATCA | TGGCTCTTGTTTGAGTCACG |
| *FOXA1* | AAGGCATACGAACAGGCACT | GTGTTTAGGACGGGTCTGGA |
| *PLAGL1* | CAGACCGGAGACCTTCTGAG | TTCTGGGCAGAAGCTCCTAA |
| *TMF1* | CATGAATCCTTGCACATTGG | GTTTCTTCGTGCTTGCCTTC |
| *RUNX2* | CGCATTCCTCATCCCAGTAT | GCCTGGGGTCTGTAATCTGA |
| *TRIM24* | GCCTAAGCAGAATCCTGTCG | GCATATGCTGGAGCCGTAAT |
| *EGR1* | CCGCAGAGTCTTTTCCTGAC | AGCGGCCAGTATAGGTGATG |
| *HOXB13* | AACTATGCCCCCTTGGATCT | CCGCCTCCAAAGTAACCATA |
| *GRHL2* | TGCCTGATCTCCACTCACAG | TCGTTCATCATCCGTGTTGT |
| *NCOR1* | AAAGTGTGGAGACCCAGGTG | TCAACGTCCACAGAGTCAGC |
| *NCOR2* | GTGTACAAAGACCGCCAGGT | AGCCACTGTCTTCCTCTCCA |
| *LMNA* | GCAGTCTCTGTCCTTCGACC | ACTGAGTCAAGGGTCTTGCG |
| *PDCD4* | ACCCTGCAGATCCTGATAACT | TTTGGACTGGTTGGCACAGT |
| *ENDOD1* | ACCATTTGCATGGGGTCGAT | CATGGTGCTAAGGGGCTCAA |
| *DHRS7* | GACCTGACGCTACTATGGGC | ACCATTGTTGACCAGAATGTCG |
| *FUS* | GGTGTTGGAACTTCGTTGCTT | TCCATAGCCTGTGTTCTGGC |
| *HDAC1* | ACTGCTAAAGTATCACCAGAGGG | CACACTTGGCGTGTCCTTTG |
| *Shh* | GGACAGGCTGATGACTCAGA | GCCCTCGTAGTGCAGAGACT |
| *β-Actin* | TTGTTACAGGAAGTCCCTTGCC | ATGCTATCACCTCCCCTGTGTG |
| *MAOA ARE* | AAGTGTTTTGGGGCACGGTTC | AATCTCTAAAGGGCAGTGTCTTTG |
| *PSA ARE* | GCCTGGATCTGAGAGAGATATCATC | ACACCTTTTTTTTTCTGGATTGTTG |
| *FKBP5 ARE* | CCCCCCTATTTTAATCGGAGTAC | TTTTGAAGAGCACAGAACACCCT |
| *NC* | ACGCTGACCATTAGAAACCTCT | GGAGAAGGTGGCTCTTTCCA |
| *YAP1 GliBS* | ACAGGGATAGCAGGGGTAGG | TAGTCACTGGAAGCCGCAAC |

**Immunofluorescence assay**

Cells were seeded on chamber slides. To determine MAOA's effect on AR nuclear translocation, control and MAOA-manipulated cells were grown in phenol red-free medium containing 5% charcoal-stripped serum (CSS) for 48 hours followed by R1881 stimulation for 6

hours. The cells were fixed with 4% formaldehyde for 10 min at room temperature (RT), washed twice with PBS containing 0.02% Tween 20, and permeabilized with 0.5% Triton X-100/PBS solution (blocking solution) for 30 min at RT. Primary antibodies against AR (N-20, Santa Cruz or D6F11, Cell Signaling, RRID: AB_10691711) or YAP1 (63.7, Santa Cruz) were incubated in blocking solution at 4$^{o}$C overnight followed by addition of secondary antibodies labeled with Alexa Fluor Plus 555 (Cat# A32732 and A32727, Thermo Fisher Scientific). Images were acquired by a Nikon Ti-E inverted microscope or a Zeiss Axio Imager M2 upright microscope using a x40 objective and analyzed for AR or YAP1 fluorescence per nucleus with inForm or HALO software.

**Luciferase reporter assay**

To validate the functionality of the *MAOA* ARE, LNCaP cells were transfected with either WT or mutated/deleted forms of *MAOA* ARE-luc together with pRL-TK to normalize for transfection efficiency. Prior to 24-hour R1881 treatment, cells were grown in phenol red-free medium containing 5% CSS for 6-8 hours. Cells were then harvested and cell lysates were assayed for relative luciferase activity by a Dual-Luciferase Reporter Assay System (Promega) following the manufacturer's instructions. To determine the effects of MAOA and YAP1 on *PSA*-luc reporter, LNCaP and C4-2B$^{ENZR}$ (shCon and shMAOA) cells were transfected with *PSA*-luc together with pRL-TK. Cells were grown in phenol red-free medium containing 5% CSS for 6-8 hours and then treated with R1881 in the absence or presence of verteporfin for another 24 hours, followed by assays of relative luciferase activity. To determine the effect of MAOA on YAP1 transactivation, LNCaP and C4-2B$^{ENZR}$ (shCon and shMAOA) cells were transfected with 8xGTIIC-luc together with pRL-TK, treated with verteporfin for 24 hours, and assayed for relative luciferase activity. To determine the effects of MAOA and Shh/Gli signaling on *YAP1* promoter, LNCaP (shCon and shMAOA) cells were transfected with a *YAP1 Gaussia* luciferase promoter-SEAP reporter. Twenty-four hours after transfection, cells were treated with cyclopamine or ethanol for another 48 hours prior to relative luciferase activity assays, calculated as the ratio of *Gaussia* luciferase activity to SEAP activity by a Secret-Pair Dual Luminescence Kit (GeneCopoeia). To validate the functionality of the GliBS identified in *YAP1* promoter, 293T cells were transfected with a WT or a mutant *YAP1* promoter-luc together with pRL-TK, treated with cyclopamine for 24 hours, and assayed for relative luciferase activity. To determine MAOA's effect on Gli-luc activity in AR-positive PC cells, control and MAOA-manipulated cells were transfected with Gli-luc together with pRL-TK and incubated for 48 hours before relative luciferase activity determination. To determine the effects of ROS or Twist1 on Gli-luc activity in AR-positive PC cells, control and MAOA-manipulated cells were co-transfected with Gli-luc and pRL-TK together with a *Twist1* expression plasmid or *Twist1* siRNAs and incubated for 24 hours. Cells were then treated with NAC for 24 hours or $H_2O_2$ for 2 hours followed by medium replenishment for $H_2O_2$ removal and subsequent 22-hour incubation before relative luciferase activity determination.

**RNA-seq and gene set enrichment analysis (GSEA)**

The total RNA of LNCaP and C4-2B$^{ENZR}$ (shCon and shMAOA) cells were extracted by RNeasy Mini Kit (Qiagen) and underwent DNase digestion following the manufacturer's instructions. RNA-seq was performed on an Illumina HiSeq 2500 at the UCLA Clinical Microarray Core. Bowtie 2 v2.1.0 was used for mapping to the human genome hg19 transcript set. RSEM v1.2.15 was used to calculate the count and estimate the gene expression level. The Trimmed Mean of M-values (TMM) method in the edgeR package was used for gene expression normalization. The RNA-seq raw sequence files reported in this study are available in the NCBI Gene Expression Omnibus database (accession number GSE161691). GSEA v4.0.3 was used to evaluate the association of MAOA expression with androgen-responsive, AR- and YAP1-dependent pathways using relevant gene sets from the molecular signature database (MSigDB v7.2).

**Cell proliferation assays**

Cells were seeded on 6-well plates (2 x $10^4$ cells/well) and treated with individual antiandrogen drugs with or without a MAOA inhibitor. Cell numbers from triplicate wells were counted by hemocytometer over a 5-day period. To determine $IC_{50}$ values of individual antiandrogen drugs in control and MAOA-KD cells, cell proliferation was determined by CellTiter 96 $AQ_{ueous}$ One Solution Cell Proliferation Assay (Promega) following the manufacturer's instructions.

**Mass spectrometry-based proteomic analysis**

The AR-interacting proteins in LNCaP (shCon and shMAOA) cells were enriched using a Pierce Co-Immunoprecipitation Kit (Thermo Fisher Scientific) following the manufacturer's instructions. For regular co-IP, a total of 4 x $10^6$ cells were collected from each replicate in the group of control or MAOA-KD cells, with 3 replicates per group, and lysed with 500 µl ice-cold IP lysis/wash buffer. An anti-AR antibody (D6F11, Cell Signaling, 1:50) or a control IgG (Cat# 2729, Cell Signaling, 1:250) was immobilized for 2 hours using AminoLink Plus coupling resin for immunoprecipitation. One and half milligram of protein lysates were immunoprecipitated with the resin at 4°C overnight to acquire co-immunoprecipitated products. The co-immunoprecipitated samples were run on SDS/PAGE followed by in-gel digestion with trypsin, and identified and quantified by mass spectrometry using the Nano LC-MS/MS platform at Creative Proteomics. The raw MS files were analyzed and searched against human protein databases using Maxquant (1.6.2.6). The fold-change cutoff was set when proteins with quantitative ratios above 1.2 or below 0.83 (1/1.2) were deemed significant. A list of proteins expressed in the nucleus and thus implicated for interactions with and potential regulatory effects on active AR were filtered out based on the information on protein subcellular localization available at the Human Protein Atlas and GeneCards databases. A literature search was further performed to retain proteins which were either (1) downregulated for binding to AR in MAOA-KD cells and positively regulate PC cell growth and/or AR activity, or (2) upregulated for binding to AR in MAOA-KD cells and negatively regulate PC cell growth and/or AR activity. Six proteins fulfilled these requirements and were subjected to further validation. Detailed protein identification and quantification information is listed in Supplementary Dataset S1.

**ROS measurement**

Intracellular ROS levels were measured according to a published protocol (35). Briefly, cells were washed with PBS and incubated with 5 µM CM-$H_2$DCFDA (Thermo Fisher Scientific) for 30 min followed by fluorescence measurement (excitation/emission wavelength: 492-495/517-527 nm) by a BioTek microplate reader.

**Co-immunoprecipitation assay**

YAP1-AR interaction in LNCaP (shCon and shMAOA) cells was determined using a Pierce Co-Immunoprecipitation Kit following the manufacturer's instructions. Cells were lysed in ice-cold IP lysis/wash buffer. An anti-AR antibody (D6F11, Cell Signaling, 1:50) or a control IgG (Cat# 2729, Cell Signaling, 1:250) was immobilized for 2 hours using AminoLink Plus coupling resin for immunoprecipitation. One microgram of total protein lysates was immunoprecipitated with the resin at 4°C overnight. After incubation, the resin was washed and proteins in the immunoprecipitates were eluted and subjected to immunoblotting analysis with antibodies against YAP1 (63.7, Santa Cruz) or AR (441, Santa Cruz).

**Supplementary References**


1. Grasso CS, Wu YM, Robinson DR, Cao X, Dhanasekaran SM, Khan AP*, et al.* The mutational landscape of lethal castration-resistant prostate cancer. Nature **2012**;487:239-43
2. Holzbeierlein J, Lal P, LaTulippe E, Smith A, Satagopan J, Zhang L*, et al.* Gene expression analysis of human prostate carcinoma during hormonal therapy identifies androgen-responsive genes and mechanisms of therapy resistance. The American journal of pathology **2004**;164:217-27
3. Wallace TA, Prueitt RL, Yi M, Howe TM, Gillespie JW, Yfantis HG*, et al.* Tumor immunobiological differences in prostate cancer between African-American and European-American men. Cancer research **2008**;68:927-36
4. Luo JH, Yu YP, Cieply K, Lin F, Deflavia P, Dhir R*, et al.* Gene expression analysis of prostate cancers. Molecular carcinogenesis **2002**;33:25-35
5. Vanaja DK, Cheville JC, Iturria SJ, Young CY. Transcriptional silencing of zinc finger protein 185 identified by expression profiling is associated with prostate cancer progression. Cancer research **2003**;63:3877-82
6. Welsh JB, Sapinoso LM, Su AI, Kern SG, Wang-Rodriguez J, Moskaluk CA*, et al.* Analysis of gene expression identifies candidate markers and pharmacological targets in prostate cancer. Cancer research **2001**;61:5974-8
7. Taylor BS, Schultz N, Hieronymus H, Gopalan A, Xiao Y, Carver BS*, et al.* Integrative genomic profiling of human prostate cancer. Cancer cell **2010**;18:11-22
8. Yu YP, Landsittel D, Jing L, Nelson J, Ren B, Liu L*, et al.* Gene expression alterations in prostate cancer predicting tumor aggression and preceding development of malignancy. Journal of clinical oncology : official journal of the American Society of Clinical Oncology **2004**;22:2790-9
9. True L, Coleman I, Hawley S, Huang CY, Gifford D, Coleman R*, et al.* A molecular correlate to the Gleason grading system for prostate adenocarcinoma. Proceedings of the National Academy of Sciences of the United States of America **2006**;103:10991-6
10. Arredouani MS, Lu B, Bhasin M, Eljanne M, Yue W, Mosquera JM*, et al.* Identification of the transcription factor single-minded homologue 2 as a potential biomarker and immunotherapy target in prostate cancer. Clinical cancer research : an official journal of the American Association for Cancer Research **2009**;15:5794-802
11. LaTulippe E, Satagopan J, Smith A, Scher H, Scardino P, Reuter V*, et al.* Comprehensive gene expression analysis of prostate cancer reveals distinct transcriptional programs associated with metastatic disease. Cancer research **2002**;62:4499-506
12. Lapointe J, Li C, Higgins JP, van de Rijn M, Bair E, Montgomery K*, et al.* Gene expression profiling identifies clinically relevant subtypes of prostate cancer. Proceedings of the National Academy of Sciences of the United States of America **2004**;101:811-6
13. Nanni S, Priolo C, Grasselli A, D'Eletto M, Merola R, Moretti F*, et al.* Epithelial-restricted gene profile of primary cultures from human prostate tumors: a molecular approach to predict clinical behavior of prostate cancer. Molecular cancer research : MCR **2006**;4:79-92
14. Setlur SR, Mertz KD, Hoshida Y, Demichelis F, Lupien M, Perner S*, et al.* Estrogen-dependent signaling in a molecularly distinct subclass of aggressive prostate cancer. J Natl Cancer Inst **2008**;100:815-25
15. Singh D, Febbo PG, Ross K, Jackson DG, Manola J, Ladd C*, et al.* Gene expression correlates of clinical prostate cancer behavior. Cancer cell **2002**;1:203-9
16. Glinsky GV, Berezovska O, Glinskii AB. Microarray analysis identifies a death-from-cancer signature predicting therapy failure in patients with multiple types of cancer. J Clin Invest **2005**;115:1503-21

17. Liu P, Ramachandran S, Ali Seyed M, Scharer CD, Laycock N, Dalton WB*, et al.* Sex-determining region Y box 4 is a transforming oncogene in human prostate cancer cells. Cancer research **2006**;66:4011-9
18. Tamura K, Furihata M, Tsunoda T, Ashida S, Takata R, Obara W*, et al.* Molecular features of hormone-refractory prostate cancer cells by genome-wide gene expression profiles. Cancer research **2007**;67:5117-25
19. Best CJ, Gillespie JW, Yi Y, Chandramouli GV, Perlmutter MA, Gathright Y*, et al.* Molecular alterations in primary prostate cancer after androgen ablation therapy. Clinical cancer research : an official journal of the American Association for Cancer Research **2005**;11:6823-34
20. Chandran UR, Ma C, Dhir R, Bisceglia M, Lyons-Weiler M, Liang W*, et al.* Gene expression profiles of prostate cancer reveal involvement of multiple molecular pathways in the metastatic process. BMC Cancer **2007**;7:64
21. Varambally S, Yu J, Laxman B, Rhodes DR, Mehra R, Tomlins SA*, et al.* Integrative genomic and proteomic analysis of prostate cancer reveals signatures of metastatic progression. Cancer cell **2005**;8:393-406
22. Robinson D, Van Allen EM, Wu YM, Schultz N, Lonigro RJ, Mosquera JM*, et al.* Integrative clinical genomics of advanced prostate cancer. Cell **2015**;161:1215-28
23. Kumar A, Coleman I, Morrissey C, Zhang X, True LD, Gulati R*, et al.* Substantial interindividual and limited intraindividual genomic diversity among tumors from men with metastatic prostate cancer. Nature medicine **2016**;22:369-78
24. Cancer Genome Atlas Research N. The Molecular Taxonomy of Primary Prostate Cancer. Cell **2015**;163:1011-25
25. Beltran H, Prandi D, Mosquera JM, Benelli M, Puca L, Cyrta J*, et al.* Divergent clonal evolution of castration-resistant neuroendocrine prostate cancer. Nature medicine **2016**;22:298-305
26. Abida W, Cyrta J, Heller G, Prandi D, Armenia J, Coleman I*, et al.* Genomic correlates of clinical outcome in advanced prostate cancer. Proceedings of the National Academy of Sciences of the United States of America **2019**;116:11428-36
27. Ren S, Wei GH, Liu D, Wang L, Hou Y, Zhu S*, et al.* Whole-genome and Transcriptome Sequencing of Prostate Cancer Identify New Genetic Alterations Driving Disease Progression. European urology **2018**;73:322-39
28. Barbieri CE, Baca SC, Lawrence MS, Demichelis F, Blattner M, Theurillat JP*, et al.* Exome sequencing identifies recurrent SPOP, FOXA1 and MED12 mutations in prostate cancer. Nature genetics **2012**;44:685-9
29. Gerhauser C, Favero F, Risch T, Simon R, Feuerbach L, Assenov Y*, et al.* Molecular Evolution of Early-Onset Prostate Cancer Identifies Molecular Risk Markers and Clinical Trajectories. Cancer cell **2018**;34:996-1011 e8
30. Wu JB, Shao C, Li X, Li Q, Hu P, Shi C*, et al.* Monoamine oxidase A mediates prostate tumorigenesis and cancer metastasis. J Clin Invest **2014**;124:2891-908
31. Jia L, Kim J, Shen H, Clark PE, Tilley WD, Coetzee GA. Androgen receptor activity at the prostate specific antigen locus: steroidal and non-steroidal mechanisms. Molecular cancer research : MCR **2003**;1:385-92
32. Sasaki H, Hui C, Nakafuku M, Kondoh H. A binding site for Gli proteins is essential for HNF-3beta floor plate enhancer activity in transgenics and can respond to Shh in vitro. Development **1997**;124:1313-22
33. Vincentz JW, Firulli BA, Lin A, Spicer DB, Howard MJ, Firulli AB. Twist1 controls a cell-specification switch governing cell fate decisions within the cardiac neural crest. PLoS genetics **2013**;9:e1003405
34. Livak KJ, Schmittgen TD. Analysis of relative gene expression data using real-time quantitative PCR and the 2(-Delta Delta C(T)) Method. Methods **2001**;25:402-8

35. Eruslanov E, Kusmartsev S. Identification of ROS using oxidized DCFDA and flow-cytometry. Methods in molecular biology **2010**;594:57-72